Title	Real-time precision pedestrian navigation solution using Inertial Navigation System and Global Positioning System
Author(s)	Yoon, Yong-Jin; Li, King Ho Holden; Lee, Jiahe Steven; Park, Woo-Tae
Citation	Yoon, Y.-J., Li, K. H. H., Lee, J. S., & Park, W.-T. (2015). Real-time precision pedestrian navigation solution using Inertial Navigation System and Global Positioning System. Advances in Mechanical Engineering, 7(3).
Date	2015
URL	http://hdl.handle.net/10220/39021
Rights	Creative Commons CC-BY: This article is distributed under the terms of the Creative Commons Attribution 3.0 License (http://www.creativecommons.org/licenses/by/3.0/) which permits any use, reproduction and distribution of the work without further permission provided the original work is attributed as specified on the SAGE and Open Access pages (http://www.uk.sagepub.com/aboutus/openaccess.htm).

Real-time precision pedestrian navigation solution using Inertial Navigation System and Global Positioning System

Yong-Jin Yoon[1], King Ho Holden Li[1], Jiahe Steven Lee[1] and Woo-Tae Park[2]

Abstract

Global Positioning System and Inertial Navigation System can be used to determine position and velocity. A Global Positioning System module is able to accurately determine position without sensor drift, but its usage is limited in heavily urbanized environments and heavy vegetation. While high-cost tactical-grade Inertial Navigation System can determine position accurately, low-cost micro-electro-mechanical system Inertial Navigation System sensors are plagued by significant errors. Global Positioning System is coupled with Inertial Navigation System to correct the errors, while Inertial Navigation System itself can be used to provide navigation solution during a Global Positioning System outage. Data from Global Positioning System and Inertial Navigation System can be integrated by extensive Kalman filtering, using loosely coupled integration architecture to provide navigation solutions. In this study, real-time low-cost loosely coupled micro-electro-mechanical system Inertial Navigation System/Global Positioning System sensors have been used for pedestrian navigation. Trial runs of Global Positioning System outages have been conducted to determine the accuracy of the system described. The micro-electro-mechanical system Inertial Navigation System/Global Positioning System can successfully project a trajectory during a Global Positioning System outage and produces a root mean square error of 9.35 m in latitude direction and 10.8 m in longitude direction. This technology is very suitable for visually impaired pedestrians.

Introduction

Global Positioning System (GPS) and Inertial Navigation System (INS) are widely used to determine position, velocity, and time (PVT) for navigation applications. GPS is a satellite-based navigation system which provides accurate positioning information. Although GPS has superior long-term performance in minimizing navigational errors, it has poor short-term accuracy when a GPS signal is unavailable. In order to overcome any temporary outage of GPS signal, GPS may be coupled with INS in navigation systems. INS has good short-term accuracy, but it has

poor long-term performance, making integration of INS and GPS system ideal. When the GPS signal is unavailable, INS can provide short-term robust

[1]School of Mechanical and Aerospace Engineering, Nanyang Technological University, Singapore
[2]Department of Mechanical and Automotive Engineering, Seoul National University of Science and Technology, Seoul, Republic of Korea

Corresponding author:
Woo-Tae Park, Department of Mechanical and Automotive Engineering, Seoul National University of Science and Technology, Seoul 139–743, Republic of Korea.
Email: wtpark@seoultech.ac.kr

navigation solutions until the GPS signal is once again available.

Kalman filtering is an optimum estimation algorithm characterized by recursive evaluation and estimation of the dynamics of the system model. Conventional Kalman filtering is a time-discrete and linear system. The time-variant stochastic error that an INS produces may result in the reduction in the observability of error states.[1] An extended Kalman filtering (EKF) assumes a nonlinear dynamic system with the presence of process and measurement noise, which is assumed to be Gaussian white noise with zero mean and known error covariance matrices.[2] An EKF integrates the measurements from GPS and INS, using position and velocity from GPS to update error states while using INS as a reference trajectory.

Proliferation of micro-electro-mechanical system (MEMS) inertial sensors would result in low-cost INS/GPS systems. The current smart phones are already equipped with multiple MEMS sensors. These include accelerometer, gyroscope, e-compass, altimeter, and humidity sensor. There was also a study using MEMS olfactory sensor[3–6] to monitor air pollution.[7] In order to use an inertial measurement unit (IMU) as an INS, the INS needs to be initialized from either coarse alignment or fine alignment.[8] Obtaining the acceleration and angular rotation from IMU, the INS mechanization equations convert the measurements into PVT information. There are two modes of INS mechanization equations which are the gimbal INS and the Strapdown Inertial Navigation System (SINS). Gimbal INS involves mounting sensors on three orthogonal rotating gimbals, while application of MEMS IMU sensors in SINS will involve mounting them on printed circuit boards without moving parts.[9]

The current smart phone technologies have its limitations in terms of GPS signal outage. For visually impaired pedestrians, expensive solutions using real-time kinetic (RTK) method are available to provide sub-meter accuracy based on subscription basis. However, based on World Health Organization's estimate of 285 million visually impaired people worldwide, more than 90% of them live in low-income settings. Our aim is to make sure of current low-cost INS/GPS system to provide alternative low-cost solution.

Traditionally, INS and GPS can be coupled via different modes, namely, loosely coupled integration and tightly coupled integration.[10] In the loosely coupled integration, PVT information from GPS updates the INS/GPS Kalman filter and feed backs the sensor error states to the INS mechanization equations.[11–16] In tightly coupled integration, it utilizes a centralized Kalman filter that integrates pseudorange and Doppler measurement from GPS and PVT information from INS.[17,18] Although tightly coupled integration is more

accurate and less sensitive to stochastic error model than loosely coupled integration, it is computationally expensive and the processing time is not suitable for low-cost MEMS application. In this work, MEMS IMU and GPS sensors will be used, and a loosely coupled INS/GPS system will be implemented to compute real-time pedestrian navigation solutions using EKF. This could potentially be used in many handheld gadgets with the potential of low-cost solution for the visually impaired.

Method

INS mathematical formulation

Coordinate frames. The linear and angular motion of one coordinate frame needs to be described with respect to one another. Measurements from the IMU need to be described as Euler's angles roll θ, pitch ϕ, and yaw ψ to be rotated to navigation frame using a rotation matrix known as attitude, C

$$C = C_x C_y C_z \tag{1}$$

$$C_x = \begin{pmatrix} 1 & 0 & 0 \\ 0 & \cos\phi & \sin\phi \\ 0 & -\sin\phi & \cos\phi \end{pmatrix} \tag{2a}$$

$$C_y = \begin{pmatrix} \cos\theta & 0 & -\sin\theta \\ 0 & 1 & 0 \\ \sin\theta & 0 & \cos\theta \end{pmatrix} \tag{2b}$$

$$C_z = \begin{pmatrix} \cos\psi & \sin\psi & 0 \\ -\sin\psi & \cos\psi & 0 \\ 0 & 0 & 1 \end{pmatrix} \tag{2c}$$

INS initialization. INS position and velocity must be initialized from external navigation systems like external INS and GPS or initialized using a pre-surveyed point. In this work, the INS is initialized from the position and velocity from GPS.

To obtain attitude of the INS ($\theta_{nb}, \emptyset_{nb}$), coarse alignment is used when the INS remains stationary. Coarse alignment is carried by a leveling process that initializes roll and pitch, followed by the gyro compassing process which initializes yaw[8]

$$\theta_{nb} = \arctan\left(\frac{-f_{ib,x}^b}{\sqrt{\left(f_{ib,y}^b\right)^2 + \left(f_{ib,z}^b\right)^2}}\right) \tag{3a}$$

$$\emptyset_{nb} = \arctan 2\left(f_{ib,y}^b + f_{ib,z}^b\right) \tag{3b}$$

where measurement from accelerometer is denoted by f_{ib}^b

During the gyro compassing process, since the INS is stationary, the only rotation a gyroscope can sense is the rotation of Earth in the *z*-direction of the Earth frame

$$\sin \psi_{nb} = -\omega_{ib,y}^b \cos \emptyset_{nb} + \omega_{ib,z}^b \sin \emptyset_{nb} \quad (4a)$$

$$\cos \psi_{nb} = \omega_{ib,x}^b \cos \emptyset_{nb} + \omega_{ib,y}^b \cos \theta_{nb} \sin \emptyset_{nb} \\ + \omega_{ib,z}^b \sin \theta_{nb} \cos \emptyset_{nb} \quad (4b)$$

where ω_{ib}^b denotes measurements from gyroscope

Using Euler's angles obtained, attitude is derived from equations (1) and (2).

INS mechanization.

INS mechanization equations update its position and velocity based on values obtained in its previous iteration (Figure 1). In the first iteration, position and velocity are obtained from GPS information and the attitude is determined from coarse alignment. The velocity of the INS can be updated as a function of gravitational vector and Earth rotation matrix in the standard World Geodetic System (WGS-84).[19] Finally, using second-order Runge–Kutta integration, the position of the INS can be computed as shown in Figure 1.

The attitude of the INS is updated as follows

$$C_b^n(+) = C_b^n(-)(I_3 + \Omega_{ib}^b \tau_i) - (\Omega_{ie}^n(-) \\ + \Omega_{en}^n(-))C_b^n(-)\tau_i \quad (5)$$

where Ω_{ib}^n is the skew-symmetric matrix of the angular rotation and τ_i is the time interval between iteration

$$\Omega_{ib}^n = [\Lambda\omega_{ib}^b] \quad (6)$$

Earth rotation matrix Ω_{ie}^n and transport matrix Ω_{en}^n were used from the study by Groves.[8]

When deriving the velocity vector ($v^n(+)$), Coriolis effect and gravitational model need to be considered such that

$$v^n(+) = v^n(-) + (C_b^n \cdot f_{ib}^b - (2 \cdot \Omega_{ie}^n + \Omega_{en}^n) \\ \times v^n(-) + \gamma^n)\tau_i \quad (7)$$

where $v^n(-)$ denotes the velocity at previous iteration and $v^n(+)$ denotes the updated velocity at current iteration.

To obtain the position vector ($p^n(+)$), velocity vector is integrated by second-order Runge–Kutta method

$$p^n(+) = p^n(-) + \frac{1}{2}(D^{-1} \cdot (v^n(-) + v^n(+)))\tau_i \quad (8)$$

where D^{-1} is a function of latitude φ, transverse radius of curvature M, and meridian radius of curvature N[19]

$$D^{-1} = \begin{pmatrix} 0 & \frac{1}{(M+h)} & 0 \\ \frac{1}{(N+h)\cdot\cos\varphi} & 0 & 0 \\ 0 & 0 & -1 \end{pmatrix} \quad (9)$$

INS error state.

INS mechanization equations in the previous section described the updated navigation state vectors without consideration of IMU error. The error state vector ($\delta \dot{x}^n$) is a 15-state vector that describes error in position, velocity, attitude, and bias in accelerometer and gyroscope[20]

$$\delta \dot{x}^n = \begin{pmatrix} \delta \dot{p}^n \\ \delta \dot{v}^n \\ \delta \dot{C}_b^n \\ \dot{b}_a \\ \dot{b}_g \end{pmatrix} \\ = \begin{pmatrix} D^{-1}\delta v^n \\ -(C_b^n f_{ib}^i) + (2 \cdot \Omega_{ie}^n + \Omega_{en}^n)\delta v^n + (C_b^n b_a) \\ -\omega_{en}^n C_b^n - C_b^n b_a \\ -\alpha b_a + w_a \\ -\beta b_g + w_g \end{pmatrix} \quad (10)$$

The gyroscope and accelerometer bias are residual stochastic errors ($\dot{b}_g, \dot{b}_a$) that can be modeled as a first-order Gauss–Markov process[8]

$$\dot{b}_g = -\alpha b_g + w_g = \begin{pmatrix} -1/\tau & 0 & 0 \\ 0 & -1/\tau & 0 \\ 0 & 0 & -1/\tau \end{pmatrix} \begin{pmatrix} b_{g,x} \\ b_{g,y} \\ b_{g,z} \end{pmatrix} + w_g \quad (11)$$

$$\dot{b}_a = -\alpha b_a + w_a = \begin{pmatrix} -1/\tau & 0 & 0 \\ 0 & -1/\tau & 0 \\ 0 & 0 & -1/\tau \end{pmatrix} \begin{pmatrix} b_{a,x} \\ b_{a,y} \\ b_{a,z} \end{pmatrix} + w_a \quad (12)$$

where α is the reciprocate correlation of time τ, w_a is the accelerometer Gauss–Markov process noise, b_a is the accelerometer instability bias, w_g is the gyroscope Gauss–Markov process noise, and b_g is the gyroscope instability bias.

INS/GPS integration architecture

Kalman filtering.

The Kalman filter is an estimation algorithm that operates recursively based on the previous estimates and prior information. It consists of two stages, the prediction stage and the update stage. The EKF assumes that the dynamic of the system model is a discrete time system.[2]

In the prediction stage, the state vector ($\hat{x}_k$) and the error covariance matrix (P_k) at the start of the current
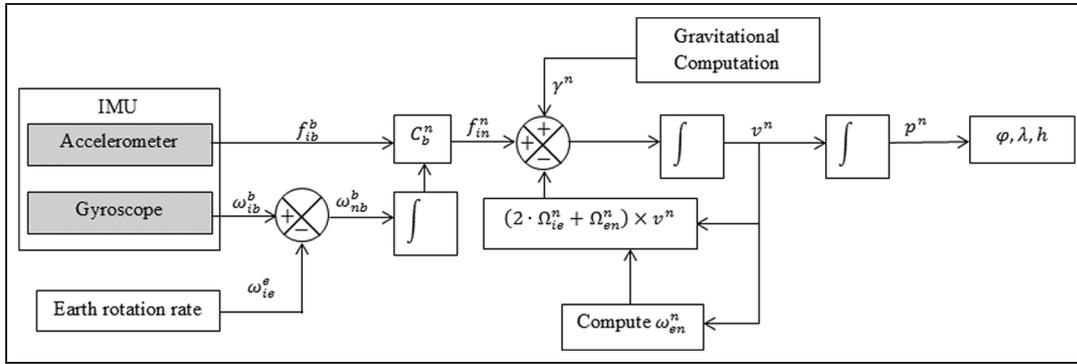
Figure 1. Schematic block diagram of INS mechanization.

epoch k are predicted based on the values obtained from the previous epoch $k-1$

$$\hat{x}_k^- = f(k, \hat{x}_{k-1}^+) \qquad (13)$$

where $f(k, x)$ is the integral of the system model found in Petovello.[21]

Error covariance matrix P_k is then propagated such that

$$P_k^- = F_{k-1}P_{k-1}F_{k-1}^T + Q_k \qquad (14)$$

In the update stage, Kalman gain is computed, state vectors are updated, and the error covariance is updated

$$K_k = P_k^- H_k^T (H_k P_k^- H_k^T + R_k)^{-1} \qquad (15)$$

where K_k denotes the Kalman gain and R_k is the noise measurement matrix.

The state vector is then updated using Kalman gain calculated at its current epoch

$$\hat{x}_k^+ = \hat{x}_k^- + K_k z_k - h(k, \hat{x}_k^-) \qquad (16)$$

where z_k denotes the measurement vector and h_k is the integral of observation matrix found in Petovello.[21]

The error covariance matrix is then updated

$$P_k^+ = P_k^- - K_k H_k P_k^- \qquad (17)$$

Prior information such as the transition matrix Φ_k, noise covariance matrix Q_k, observation matrix H_k, shaping matrix G_k, and measurement noise matrix R_k need to be determined before the start of the experiment.

The transition matrix Φ_k can be expanded using Taylor's series expansion. Ignoring higher order terms, the transition matrix can be expressed as

$$\Phi_k = \exp(F_{k-1}\tau_i) \approx I + F\tau_i \qquad (18)$$

where full expression of system matrix F can be found in Bhatti.[16]

Process noise matrix Q can be defined as power spectral density if the random velocity walk error and random angular walk error such that

$$Q_k = diag\left(n_{rg}^2 I_3 \quad n_{ra}^2 I_3 \quad 0_3 \quad n_{bad}^2 I_3 \quad n_{bdg}^2 I_3 \right)\tau_i \qquad (19)$$

where I_3 is a 3×3 identity matrix, n_{rg}^2 is the power spectrum density (PSD) of angular random noise, n_{ra}^2 is the PSD of the velocity random walk, n_{bad}^2 is the PSD of bias instability of accelerometer, and n_{bgd}^2 is the PSD of bias instability of gyroscope.

The observation matrix H_k can be expressed as

$$H_k = \begin{pmatrix} 0_3 & 0_3 & -I_3 & 0_3 & 0_3 \\ 0_3 & -I_3 & 0_3 & 0_3 & 0_3 \end{pmatrix}_k \qquad (20)$$

The shaping matrix G_k rotating the system noise of the INS to Earth frame can be expressed as

$$G_k = \begin{pmatrix} C_b^n & 0_3 \\ 0_3 & C_b^n \\ 0_{9 \times 3} & 0_{9 \times 3} \end{pmatrix} \qquad (21)$$

Noise measurement matrix R_k is the mean square of measurement noise which is assumed to be additive white Gaussian noise with zero mean

$$R_k = E(v_k v_k^T) \qquad (22)$$

In the state-space model, error of the state vector and measurement vector is calculated.

System dynamic model of the EKF can be expressed as

$$\dot{x}_k = f(x_k) + G_k w_k \qquad (23)$$

where w_k is the process noise of INS.

Measurement model of the EKF can be expressed as

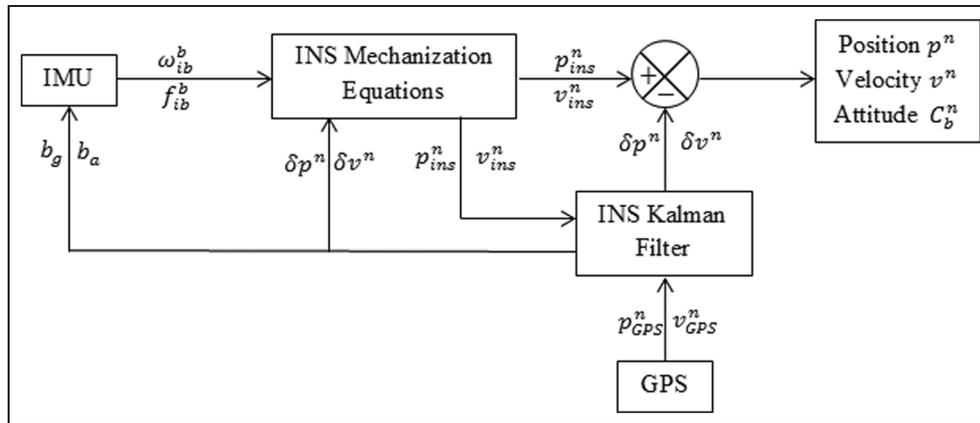$$z_k = h(x_k) + v_k \qquad (24)$$

Figure 2. Schematic block diagram of INS/GPS loosely coupled integration.

where v_k is the measurement noise of the INS.

In the INS/GPS system, the measurement vector z_k can be expressed as the difference of the measurement between the INS and GPS in equation (25)

$$z_k = \begin{pmatrix} p_{ins}^n - p_{gps}^n \\ v_{ins}^n - v_{gps}^n \end{pmatrix} \qquad (25)$$

Loosely coupled INS/GPS. After INS mechanization equations, the state vector will be calculated. Combining PVT information from GPS and the state vector of the INS into the Kalman filter, the position and velocity can be predicted and updated. When there is no GPS signal, the INS Kalman filter will predict the position and velocity based on state space model of the INS (Figure 2).

The GPS device processes the PVT information in standard National Marine Electronics Association (NMEA) signals[19] which will then be processed into geodetic location and velocity-over-ground. Once the GPS device receives a lock from the satellite,[19] the PVT information will be used to initialize the INS mechanization equations.

The loosely coupled INS/GPS architecture cascades the GPS information into the centralized INS/GPS Kalman filter with the INS state vectors to derive INS/GPS position and velocity based on the state system model used in equations (23) and (24). In the closed-loop set-up, the IMU bias will be fed back to correct the INS error states used in equations (11) and (12).

Modeling of INS error

To derive Q_k from equation (19), the Allan Variance method[21] was implemented to determine acceleration and angular random walk and the bias instability. The IMU was placed on a flat surface stationary for 5 h at sampling rate of 10 Hz without external environmental

Table 1. Velocity random walk and bias instability of accelerometer.

Accelerometer	Velocity random walk ((m/s)/$\sqrt{h}$)	Bias instability (mg)
x-axis	0.447	0.396
y-axis	0.360	0.465
z-axis	0.286	1.066

Table 2. Angular random walk and bias instability of gyroscope.

Gyroscope	Angular random walk ($°/\sqrt{h}$)	Bias instability ($°/s$)
x-axis	0.409	0.676
y-axis	0.335	1.319
z-axis	0.451	1.410

disturbance to the system.[10] The data were processed in MATLAB©, where the PSD of the gyroscope and accelerometer random walk and bias instability can be determined (Tables 1 and 2).

To derive R_k from equation (22), the data from INS and GPS were collected at a stationary platform for 1 h without GPS outage to determine v_k from equation (24). The data collected were processed using MATLAB.

Experiment procedure and hardware selection

The purpose of this study was to implement a pedestrian INS/GPS system. To verify the accuracy of the INS/GPS system, the experiment was conducted in clear weather on a 400-m *circular* stadium track to determine the accuracy of the system. To simulate GPS outage, the daughterboard of the GPS device was switched off for 20 s at time 120 s (Figure 3).
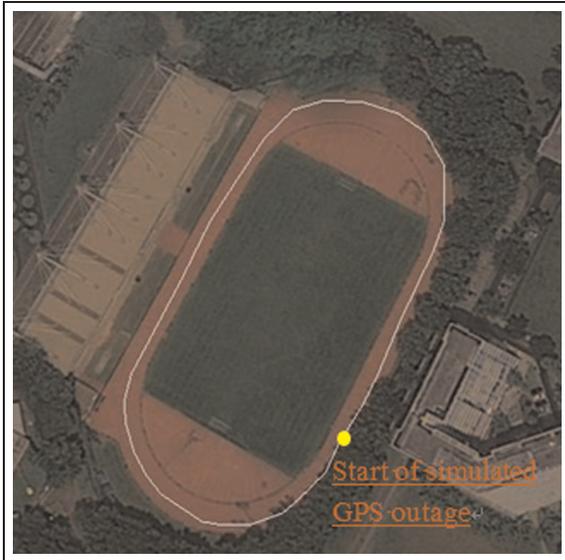
Figure 3. A Google Earth image of the path taken during the experiment conducted on lane 4 of a stadium track. The yellow dot is the start of the simulated GPS outage 120 s after the start of the experiment. A GPS outage was simulated by switching the GPS daughterboard off for 20 s.

The hardware implementation was performed in three stages. The first stage consists of the design and calibration of the commercially off-the-shelf IMU. The second stage was coding and implementing EKF onto the INS/GPS system and the third stage is to verify the performance of the INS/GPS system. The IMU digital combo (SparkFun, USA) that consists of a tri-axial accelerometer ADXL-345 (Analog Device, USA) and tri-axial gyroscope ITG-3200 (Invensense, USA) is used. IMU measurements are updated at 10 Hz. The low-cost GPS module is a u-blox LEA-5H GPS (u-blox, Switzerland). The GPS format is in NMEA format and it updates at 2 Hz. The microcontroller used is
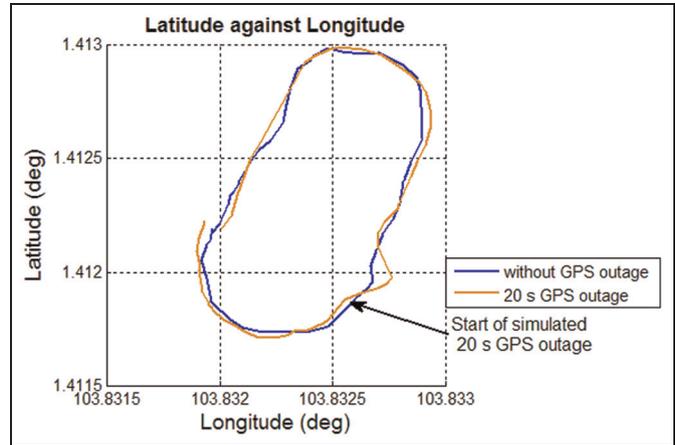

Figure 4. Comparison of the two trajectories (solid blue line: without GPS outage and solid brown line: with 20 s GPS outage) taken with an active GPS and during a simulated 20 s GPS outage after the start of the experiment.

the Arduino Due (Arduino, Italy). The Arduino Due is a 32-bit ARM core running at 84 Hz.

Results and discussion

Experimental data collected were processed in MATLAB/Simulink Kalman filter, and the geodetic data were processed using MATLAB mapping tool.

Figure 4 shows the comparison of the two trajectories taken with an active GPS and during a simulated 120-s GPS outage after the start of the experiment. During the GPS outage, there was a drift from the original trajectory, indicating that INS Kalman filter was predicting the geodetic location (Figure 4). The drift of the trajectory was caused by the bias instability of the MEMS IMU sensor.

From Figures 5 and 6, at time 120 s, there are the latitude and longitude errors increased during the time
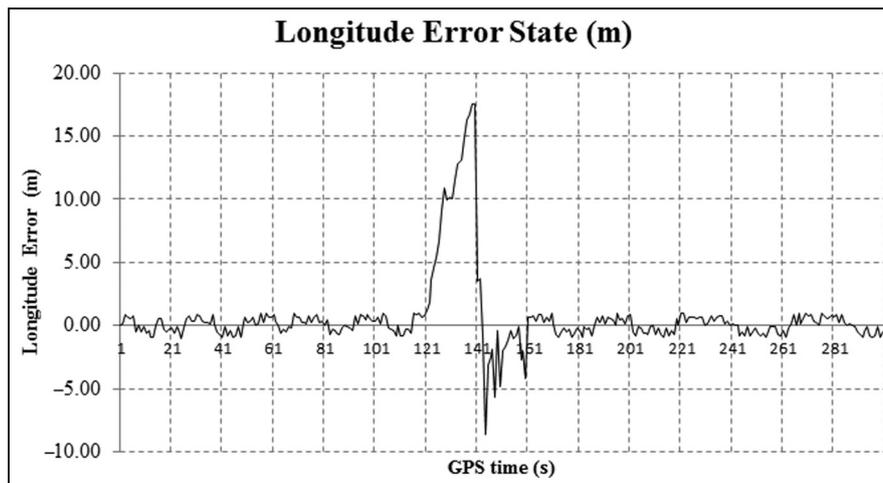

Figure 5. The longitude error state (*y*-axis) according to GPS time (*x*-axis) of the INS/GPS system.
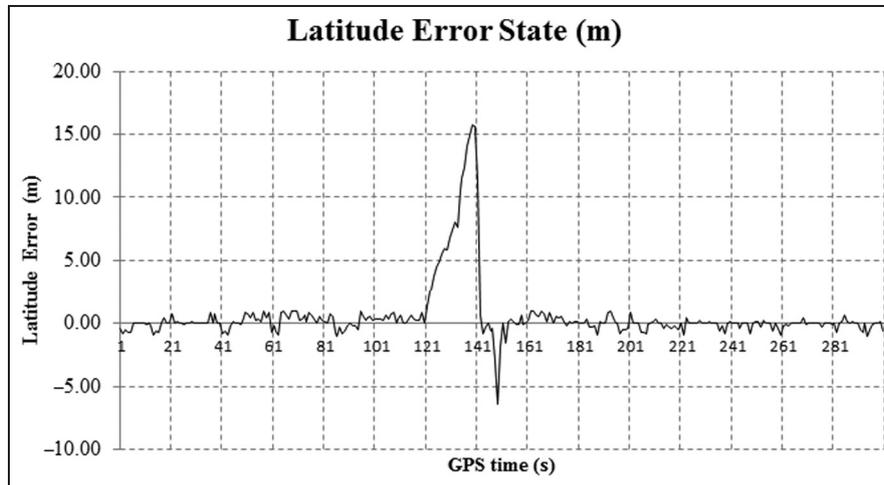
Figure 6. The latitude error state (*y*-axis) according to GPS time (*x*-axis) of the INS/GPS system.

duration of the GPS outage. When the GPS signal was cut, the error of the INS/GPS increased due to sensor error. At instances other than the simulated GPS outage, there were also latitude and longitude errors caused by the design of the priori error covariance matrix. The priori error states Q_k and R_k were computed before the experiment and assumed to be constant white noise.[8] Since the priori error matrix was not updated real-time, some accuracy of the readings will degrade.

When the GPS signal was lost, the INS Kalman filter predicted the position based on the state-space model. From Figure 4, after GPS outage has been simulated, the path deviated from the original trajectory without GPS outage. The deviation occurred as the IMU error was not corrected given in equations (11) and (12). From the state-space model given by equation (24), error of the state vector increased without the input of GPS position and velocity.

There was also deviation from the original path when there was no GPS outage; the deviation of the path can be attributed to the design of the priori state matrix like measurement noise covariance matrix R_k and process noise covariance matrix Q_k. In this study, the priori states have been assumed to fit the INS error model; this method can save computational effort and reduce processing time.[8] So, deviations in the INS noise covariance model will then reduce the accuracy of the INS/GPS Kalman filter. This problem can be overcome by replacing the EKF with adaptive Kalman filter (AKF).[22–24] The AKF model assumes a nonlinear covariance matrix that is dependent on the state vector; however, the AKF mode is computationally expensive. Neural network architecture like Fuzzy–Padé controller[25] is able to learn and train the system dynamic and error model. It performs better than the EKF, but it is computationally too expensive for real-time applications.

Table 3. RMS error at different duration of GPS outage.

GPS outage (s)	Latitude RMS error (m)	Longitude RMS error (m)
1	0.82	0.78
2	2.10	1.01
5	3.08	2.79
10	5.25	6.43
20	9.35	10.8

GPS: Global Positioning System; RMS: root mean square.

The results showed that the application of INS/GPS was able to produce reliable navigation solutions similar to previous loosely coupled INS/GPS Kalman filter integration.[11–14] From Table 3, the root mean square (RMS) error produced by the MEMS INS/GPS system was higher than RMS error produced by tactical-grade MEMS INS/GPS system during a GPS outage.[26] The low-cost MEMS IMU was able to produce reliable navigation solutions during short interval of GPS outages which was less than 10 s. Future work for this application is to couple the INS/GPS system with a piezoelectric energy harvester under low level of vibration.[27] This application can be applied to visually impaired pedestrians navigating in alleys and nature with trees and vegetation. Limitation due to GPS outage can be overcome by coupling the device with the IMU sensors. A summary of the advantages and disadvantages of various technologies is listed as below (Table 4).

Conclusion

In this article, the proposed INS/GPS system was successfully implemented with reliable results. This article

Table 4. Comparison of various methods for visually impaired pedestrian's navigation.

Methods	Advantages	Disadvantages
GPS	Well-established and found in most smart phones and electronic gadgets	GPS signal outage and disruption of service
GPS–RTK	Sub-meter accuracy with precision	Subscription basis and possible for the lower income
GPS–INS tightly coupled	Good accuracy	Computational expensive and required faster signal processing capability in handheld devices
GPS–INS loosely coupled	Fast and reasonable accuracy as proven in this work	Not as accurate as GPS–RTK

GPS: Global Positioning System; RTK: real-time kinetic; INS: Inertial Navigation System.

provided a mean for real-time implementation of a loosely coupled INS/GPS system using low-cost off-the-shelf sensors. This article used the EKF to aid INS with GPS measurements to compensate for IMU bias and to predict INS position and velocity during GPS outage. Based on Kalman filter noise behavior, the noise covariance and measurement noise matrices were determined. Real-time navigation algorithm was performed on the microcontroller. Experimental test and results were presented to validate the accuracy of the INS/GPS system. Based on this study, smart pedestrian positioning system can be developed with the integration of MEMS-based inertial sensors and GPS using existing low-cost solutions. This is especially useful for the hundreds of millions of visually impaired people worldwide, especially the lower income.

Declaration of conflicting interests

The authors declare that there is no conflict of interest.

References

1. Hong S, Lee MH, Chun H-H, et al. Observability of error states in GPS/INS integration. *IEEE Trans Veh Technol* 2005; 54(2): 731–743.
2. Haykin S. *Kalman filtering and neural networks*. New York: John Wiley & Sons, 2004.
3. Heidari A, Yoon Y-J, Lee MI, et al. A novel checker-patterned AlN MEMS resonator as gravimetric sensor. *Sensor Actuat A: Phys* 2013; 189: 298–306.
4. Heidari A, Yoon Y-J, Park MK, et al. High sensitive dielectric filled lame mode mass sensor. *Sensor Actuat A: Phys* 2012; 188: 82–88.
5. Heidari A, Yoon Y-J, Son HS, et al. Simulation based design of disk resonator based biosensors under fabrication uncertainty. *J Mech Des* 2012; 134(4): 041005.
6. Heidari A, Yoon Y-J and Choi H-J. Analysis and design of a high performance and low cost bio-mass sensor based on the radial contour mode disk resonator. *Microelectron Eng* 2011; 88(8): 1730–1732.
7. Honicky R, Brewer EA, Paulos E, et al. N-smarts: networked suite of mobile atmospheric real-time sensors. In: *Proceedings of the 2nd ACM SIGCOMM workshop*, Seattle, WA, 17–22 August 2008, pp.25–30. New York: ACM.
8. Groves PD. *Principles of GNSS, inertial, and multi-sensor integrated navigation systems*. Boston, MA: Artech House, 2007.
9. Titterton DH. *Strapdown inertial navigation technology*. Stevenage: Institution of Electrical Engineers, 2004.
10. Woodman OJ. *An introduction to inertial navigation*. Technical report number 696, University of Cambridge, Cambridge, UK, 2007.
11. Sahawneh LR, Al-Jarrah MA, Assaleh K, et al. Real-time implementation of GPS aided low-cost strapdown inertial navigation system. *J Intell Robot Syst* 2011; 61(1–4): 527–533.
12. Hjortsmarker N. *Experimental system for validating GPS/INS integration algorithm*. Master's Thesis, Lulea University of Technology, Lulea, 2006.
13. Gupta A, Evani SSS and Koipillai RD. A Kalman filtering approach for integrating MEMS-based INS and GPS for land vehicular application. *India National Conference on Communications*, Kanpur, India, 2007.
14. Aggarwal P. *MEMS-based integrated navigation*. Boston, MA: Artech House, 2010.
15. Skog I and Händel P. Calibration of a MEMS inertial measurement unit. In: *XVIII IMEKO World Congress*, Rio de Janeiro, Brazil, 17–22 September 2006.
16. Bhatti U. Failure modes and models for integrated GPS/INS systems. *J Navigation* 2013; 60(2): 327–348.
17. Yi Y. Tightly-coupled GPS/INS integration using unscented Kalman filter and particle filter. In: *Proceedings of the 19th international technical meeting of the satellite division of the institute of navigation (ION GNSS)*,

Fort Worth, TX, 26–29 September 2006, pp.2182–2191. Manassas, VA: The Institute of Navigation.

18. Jan W and Trommer GF. Tightly coupled GPS/INS integration for missile applications. *Aerosp Sci Technol* 2004; 8(7): 627–634.

19. Grewal MS. *Global positioning systems, inertial navigation and integration*. New York: John Wiley & Sons, 2001.

20. Shin E-H. *Accuracy improvement of low cost INS/GPS for land applications*. MSc Dissertation, University of Calgary, Calgary, AB, Canada, 2001.

21. Petovello MG. *Real-time integration of tactical-grade IMU and GPS for high-accuracy positioning and navigation* PhD Dissertation, University of Calgary, Canada, 2003.

22. Mohamed AH and Schwarz KP. Adaptive Kalman filtering for INS/GPS. *J Geodesy* 1999; 73(4): 193–203.

23. Sasiadek JZ, Wang Q and Zeremba MB. Fuzzy adaptive Kalman filtering for INS/GPS data fusion. In: *Proceedings of the 2000 IEEE international symposium on intelligent control*, Rio Patras, 17–19 July 2000. New York: IEEE.

24. Loebis D, Sutton R, Chudley J, et al. Adaptive tuning of a Kalman filter via fuzzy logic for an intelligent AUV navigation system. *Control Eng Pract* 2004; 12(12): 1531–1539.

25. Abedinnasab MH, Yoon Y-J and Saeedi-Hosseiny MS. High performance fuzzy-padé controllers: introduction and comparison to fuzzy controllers. *Nonlinear Dynam* 2012; 71(1): 141–157.

26. Liu H, Nassar S and El-Sheimy N. Two-filter smoothing for accurate INS/GPS land-vehicle navigation in urban centers. *IEEE Trans Veh Technol* 2010; 59(9): 4256–4267.

27. Yoon Y-J, Park W-T, Li KH, et al. A study of piezoelectric harvesters for low-level vibrations in wireless sensor networks. *Int J Precis Eng Manuf* 2013; 14: 1257–1262.

Appendix I

Notation

C	attitude
f^b	specific force measured by accelerometer
F_k	system dynamics matrix
h	heading
H_k	observation matrix
K_k	Kalman gain
p^n	position in North–East–Down (NED) direction
P_k	error covariance matrix
Q_k	spectral density matrix
R_k	noise measurement matrix
v^n	velocity in North–East–Down direction
x^n	state vector
δx^n	error in state vector
θ	pitch
λ	longitude
φ	latitude
ϕ	roll
Φ_k	transition matrix
ψ	yaw
ω^b	angular motion measured by gyroscope